

LHC circulating beam accidents for near-beam detectors

R.B. Appleby

Abstract

The LHC stored beam contains 362 MJ of energy at the top beam energy of 7 TeV, offering considerable risk to the accelerator components and detectors of the machine. In this work, beam accident scenarios for the stored beam are considered which can present a danger for the near-beam moveable detectors of LHCb and TOTEM. Failures of the circuits powering dipoles and quadrupoles and impact of the beam are calculated, along with the possible quench of superconducting magnets. It is shown the moveable detectors are in the shadow of the collimation system, relying on the correct positioning and phase of collimating elements. The possible impact of rescattered protons is discussed. Also considered is the danger to the near-beam experiments from local closed bumps, which can significantly reduce the available aperture at the near-beam experiments and cause direct beam strike if unmonitored. Finally, conclusions are drawn, along with prospects for future studies.

CERN, EN Department

1 Introduction

The design luminosity of the LHC ($10^{34} \text{ cm}^{-2} \text{ s}^{-1}$ in 7 TeV p-p mode) requires 2808 bunches, of $1.15 \cdot 10^{11}$ proton per bunch, in each of the two beams. This results in a beam energy of 362 MJ, which is enough to cause considerable damage to the normal and superconducting elements of the machine. Furthermore the beam energy density is three orders of magnitude above currently operating machines. A complex system of machine protection has been designed to protect the machine, including beam loss monitors, current monitors, quench monitors and so on, which are connected to a beam dump and interlock system. Further details of these systems and an overview of LHC machine protection can be found in [1]. Of particular concern for machine protection is changes in magnetic fields around the ring arising from equipment failures and quenches, which can cause abnormal beam dynamics of the circulating beam and potential losses in elements of the machine or experiments. The impact of these circuit and magnet failures on the circulating beam can be characterised in terms of a time constant for the change, which sets the speed of the failure and which of the machine protection systems detects it first, with beam evolution calculations in the time domain. Study of the warm separation dipole failure, evolution of the stored beam and protection of the machine has been studied in [2], and some studies will form part of [3].

In this report we consider the possible stored beam accident scenarios arising from magnet circuit failures and quenches which could impact the near-beam experiments. In particular, the near-beam moveable detectors of TOTEM, with the distance of closest approach being 10σ , and the VELO of LHCb will be considered. For each of these experiments, the worst possible magnet circuit failures and quenches will be studied, with the time evolution of the beam calculated over many turns to assess the risk to the detectors, speed of loss and the loss patterns. These studies also consider the impact of local closed bumps on the experiment, where local corrector magnets can create a closed bump across an experimental region. These bumps reduce the available aperture of the machine and could potentially cause direct beam strike.

The layout of this report is as follows. In section 2 the circuit and magnet layout of the LHC will be described, with the impact on the beam accident scenarios considered. This will include a discussion of the time decay of magnets under a quench, along with the associated quench protection circuits. The method of beam evolution calculation will be discussed in section 3. The results for the TOTEM detectors for all scenarios will be described in section 4 for both 7 TeV and 450 GeV stored beams with collision optics, along with local bumps across TOTEM. The LHCb VELO results will be discussed in section 5 for a 450 GeV stored beam with collision optics and for local bumps. Finally, the conclusions and prospects for further work will be in section 6.

2 Circuit and quench models

In this section, the circuit layout of the LHC relevant to this work is described, along with the current decay models used for a circuit failure and a magnet quench.

2.1 The circuit models

The magnets in the LHC are connected in series, with a set of related magnets powered by a single circuit. For example, the warm separation dipoles for ATLAS (D1) are connected together in series in a circuit called RD1.LR1 (R is the code for electrical circuits). The implication is that a circuit failure results in the field decay of all magnets in that circuit. The list of circuits, along with the magnets they contain, can be found in

the LHC layout database [4]. The failure of a circuit results in the decay or rise of the currents in the magnets powered (a decay from a technical failure and a rise from a circuit being anomalously driven to maximum voltage), which is modelled as a RL circuit in the absence of experimental data on the current change. The data on the real current change exists [5] and its analysis and beam dynamics effects will be studied in future work. The time constant for the RL model is found on the data page for the circuit. The power circuits are connected to power converters, which provides the voltage across the circuit, and the peak voltage is taken to be the maximum steady voltage of the power converter, and corresponds to the applied voltage for a 7 TeV beam. In this work the worst case circuit failure is considered, which corresponds to a current decay from the top power converter voltage to zero if the circuit is operating for a 7 TeV beam, and an increase from the 450 GeV nominal voltage (reduced from the top voltage by a factor of 7000/450) to the top voltage of the power converter for a 450 GeV beam. In these studies, the top voltage is increased by a safety factor of 10%.

The exponential decay or rise of a circuit is modelled by a scaled exponential,

$$I(t) = \left[1 - \exp\left(-\frac{t}{\tau}\right)\right] \left(\frac{V_f}{V_n} - 1\right), \quad (1)$$

where τ denotes the time constant of the change, V_n denotes the nominal (initial) voltage and V_f denotes the final voltage. The time constant for a circuit is found in the layout database for a circuit failure, and the maximum voltage in a circuit is taken from the maximum steady voltage of the associated power converter, plus a 10% safety factor. As previously explained, the nominal voltage for a 7 TeV beam is taken to be the top voltage, and the nominal voltage for a 450 GeV beam is taken to be the steady voltage with a factor of 7000/450. The changing current is applied to the integrated strength of all magnets in the circuit.

2.2 Magnet quenches

The quench of a magnet is modelled by Gaussian decay of the current, with a temporal width σ of 200 ms at 7 TeV [1] and 2000 ms at 450 GeV, and decay factor defined as

$$I(t) = \exp\left(-t^2/2\sigma^2\right). \quad (2)$$

The long width means losses from quenches are very slow at 450 GeV. The decay of the current produces a corresponding decay of the integrated strength of the quenched magnet. At the same time, the magnets in the same circuit as the quenched magnet start to decay exponentially, as the quench protection circuit activates to protect the magnetic systems. This decay has a time constant of 40s for quadrupoles and 104s for main superconducting bend magnets [6], and results in a corresponding drop in integrated strength of all magnets in the circuit according to equation 1. The decay of the current in the protection circuit follows the decay of the power converter voltage, with the top voltage being set to the maximum steady voltage from the power converted, plus a safety factor of 10%.

3 Time-dependent beam dynamic methods

The calculation of the time evolution of the LHC stored beam under the change of a powering circuit requires a turn-to-turn based time-dependent particle tracking code. These time-dependent studies of beam evolution and proton loss were performed using

MADX [7], with the LHC optics v6.5. The inputs to the calculations are the current optics, the settings of the collimators and the dynamics of the field changes. The computational steps followed were

1. The one-turn machine optics are calculated, and the phase 1 collimators positioned around the closed orbit. A Gaussian beam is created at the observation point. The lattice is assumed to be error-free at $t=0$. A single turn of the machine is tracked to ensure a matched beam.
2. The time step is computed in terms of turn number, and the change in circuit current is computed for all changing circuits and quenched magnets. The new integrated strengths of all elements in the circuits is applied.
3. One turn of the machine is tracked, storing the particle distribution after the turn at the observation point in a global MADX tfs table. A complete description of all particle losses, including turn number, is stored in a global tfs loss table.
4. The turn number is incremented, and the procedure is iterated from step 2.

This procedure allows a time-dependent study of the beam dynamics, proton loss evolution and time dependent loads on collimators. The tracking was performed on a turn-by-turn basis with up to 10^5 tracked protons. The data handling and plotting was performed with root [8].

4 TOTEM

In this section accident scenarios for the roman pots of TOTEM [9] in LSS 5 are considered, with a 7 TeV or a 450 GeV stored beam, considering cases of dipole circuit failure, main dipole quench, quadrupole circuit failure and quadrupole quench. An analysis of local bumps across the TOTEM pots is also considered.

The TOTEM roman pot installation around point 5 consists of two sets of silicon detectors, housed in roman pots, and located symmetrically around the IP at 147m (145m to 149m) and 220m (216m and 220m). The 147m station is located after the TAN absorber and before the D2 separation dipole. The 220m station is located immediately before Q6. Note there is a third location at 180m, with space reserved, which may be used later. At both the 147m and 22m locations, there are two roman pot stations (separated by a distance of 4m at 220m and less than 4m at 147m) allowing precise determination of proton angle. Each roman pot station consists of two units with each unit consisting of two pots, that move vertically and horizontally. The distance of approach of the window of the roman pots to the beam is constrained by the beam halo and the setting of absorbers, and will be a maximum of 10σ from the beam. For the nominal collision optics, this is equivalent to a closest physical distance of 1mm for the horizontal pots in the 220m station. The roman pots containing vertical detectors have detectors above and below the beam (a symmetrical arrangement), whereas pots containing a horizontal detector only have a detector on the outer side of the ring (an asymmetrical arrangement).

The details of machine optics are crucial to the success of TOTEM, and special sets of high β^* optics have been developed. However the studies in this report are done for nominal machine conditions with $\beta^*=0.55\text{m}$ at 7 TeV and $\beta^*=10\text{m}$ at 450 GeV, and can be redone once all the information for high β^* running conditions becomes available.

4.1 Circulating beam failures for 7 TeV collision optics

In this subsection, the circulating beam failures for TOTEM with 7 TeV collision optics are considered.

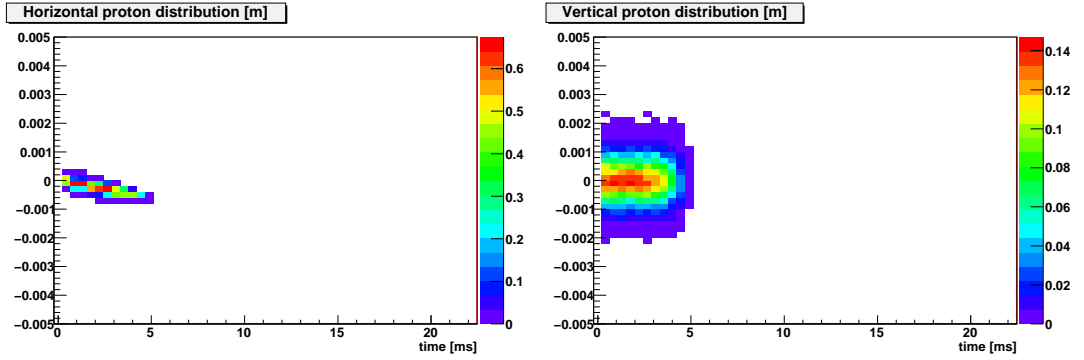


Figure 1: The horizontal and vertical proton distribution (in normalised units) at the TOTEM roman pots as a function of time, for a circuit error in RD1.LR1. The calculation was made for a 7 TeV stored beam with nominal collision optics. The nearest TOTEM pot to the beam is at 1mm in the horizontal plane in this plot.

4.1.1 Separation dipole circuit failure in LSS 1 and 5

The circuit RD1.LR1 drives the warm separation dipole D1 in point 1, on both sides of the IR. The warm separation dipoles were first identified as troublesome for beam accidents in [2]. This magnet is warm for points 1 and 5, and hence has a shorter time constant than the colder separation dipoles at other locations around the LHC, and the horizontal phase differences between the D1 magnets at point 1 and the 2nd TOTEM detector station is -238° and -58° for the left and right magnets respectively (31.65 for the left D1 32.15 for the right D1, in units of 2π , and the 220m station being at 64.21). Note the phase difference between the 150m and 220m TOTEM stations is 40° (the 150m station is at 64.2 and the 220m station is at 64.31). The circuit decay is modelled with an exponential time constant of 2.038s [4], with the voltage decaying from the top voltage of 1045 V (950 V with a 10% safety margin) to zero. The decay of the D1 bend angle will result in an orbit distortion $x(s)$ around the ring due to angular kick θ_j at position j , according to [10]

$$\Delta x(s) = \frac{\sqrt{\beta(s)\beta_j}}{2 \sin(\pi Q)} \theta_j \cos(|\Psi(s) - \Psi_j| - \pi Q), \quad (3)$$

where $\beta(s)$ denotes the β -function at position s and Q denotes the tune (the horizontal tune is 64.31 for collision optics).

Figure 1 shows the horizontal and vertical orbit distortion in the TOTEM 220m roman pots, for a worst-case failure of circuit RD1.LR1. The proton densities are shown as a function of time, with the failure occurring at $t=0$, for a stored 7 TeV beam with collision optics ($\beta^*=0.55\text{m}$). Hence the crossing angles and spectrometer dipoles are turned on, the separation bumps are turned off, and the phase 1 collimator apertures are set to the values for the phase 1 collimation scheme, which are given in the appendix of this report. The calculations show the beam orbit rapidly distorts in the horizontal plane, deviates to negative x (as the beam is not brought back to the nominal orbit at larger x as the magnet turns off) and is lost after around 5ms. The beam does not reach the 147m or 220m roman pot apertures in this time, within the tail population accuracy of the simulation. Figure 2 shows the location of the proton losses around the ring, with $s=0$ corresponding to the 220m roman pots. The principle loss spike occurs at the primary collimator TCP.B6L7.B1, positioned at 6σ , in the Betatron cleaning section and located

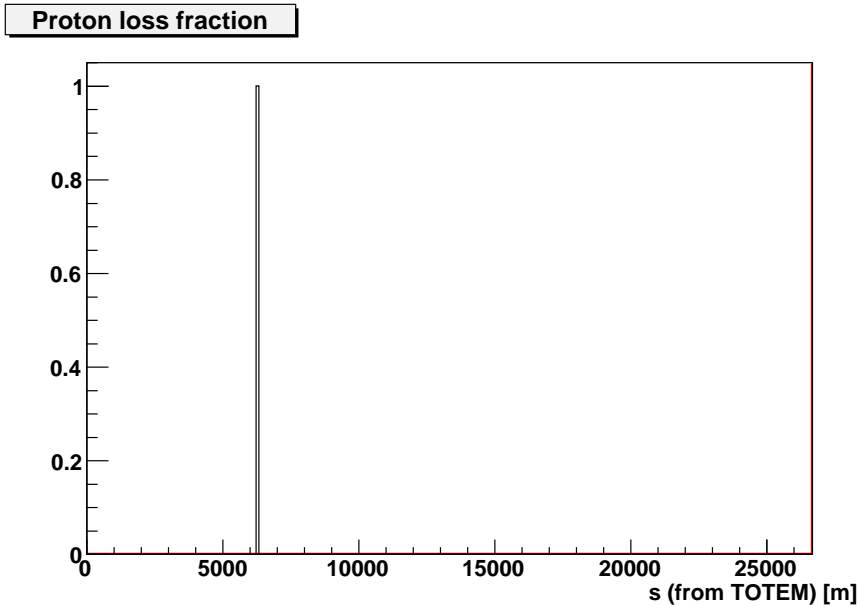


Figure 2: The proton loss map around the ring for a circuit error in RD1.LR1. The calculation was made for a 7 TeV stored beam with collision optics. The major loss spike corresponds to loss on a primary collimator.

30° in phase after TOTEM. The amount of orbit distortion and the position of the loss on the primary collimators is consistent with [2]. This collimator is at a phase advance of 268°/88° from the D1 magnets at left and right of point 1, and so the angular kick is translated into a large orbit excursion at this quadrupole. There are a series of collimators positioned after TCP.B6L7.B1, with $\sim 0^\circ$ and 180° phase advances, which will catch any protons re-scattering from this collimator and hence the probability of such a proton surviving to an orbit excursion of 10σ at the TOTEM roman pots is small. This conclusion can be checked in future work, by modelling the proton rescattering at the primary collimations with Sixtrack.

Therefore the TOTEM roman pots are in the shadow of the collimation system for a 7 TeV stored beam if the circuit RD1.LR1 fails, provided the primary collimators are correctly positioned. The calculation is done for an ideal orbit within the machine, which should not change the conclusions as all near-beam devices and collimators are positioned with respect to the machine actual closed orbit. The impact of machine errors is discussed in [3].

The calculation results for the failure of the circuit RD1.LR5, powering the separation dipoles (D1) in point 5 immediately preceding the TOTEM roman pot stations are shown in figure 3. For this case the time constant of the exponential decay is taken to be 2.26s [4], with the same top voltage as point 1. The effect on the orbit at TOTEM is expected to be largest from a failure of this circuit, as the element MBXW.A4R5 in the right D1 at point 5 (D1.R5) has the largest value of the distortion at TOTEM, according to equation 3, in the entire LHC ring. The beam orbit change is the same as for the failure of RD1.LR1 in point 1, and the loss is confined to the primary collimator TCP.B6L7.B1, so the beam does not reach the 147m or 220m roman pot apertures. The loss profile can be seen in figure 4. Again, the amount of orbit distortion and the position of the loss is consistent with [2], where losses are seen on a primary collimator in the Betatron cleaning

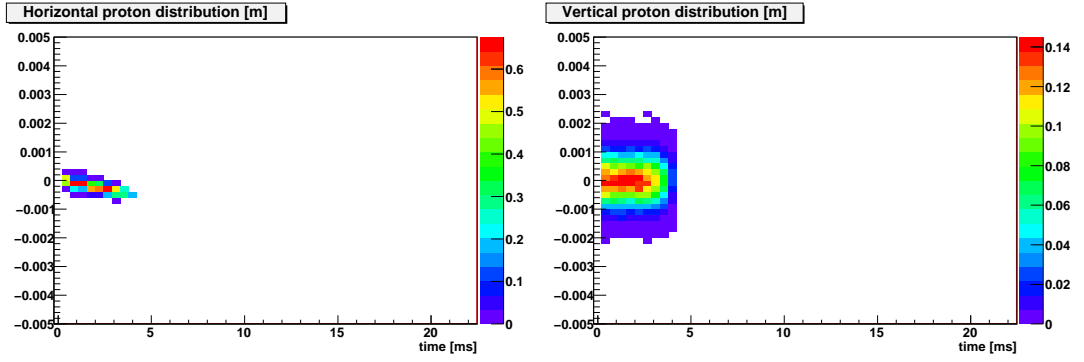


Figure 3: The horizontal and vertical proton distribution at the TOTEM roman pots as a function of time, for a circuit error in RD1.LR5 (The separation dipoles immediately preceding the TOTEM roman pots). The calculation was made for a 7 TeV stored beam with nominal collision optics.

section within a few ms.

4.1.2 Main dipole quench in sector 45

The possible danger to TOTEM from magnet failures arises from closed orbit distortion from short time constant magnet failures. A particular concern is the quench (with time constant 200ms) of a main dipole with a phase which maximises the cosine term in equation 3, which would cause a large distortion at TOTEM. One such magnet is MB.B12L5.B1, which is in the circuit RB.A45 and is at the phase before TOTEM leading to a large cosine term. The bend is positioned 457m before IP5. The quench has been modelled as a Gaussian decay with time constant 200ms, and the protection circuit decay has been modelled with an exponential time constant of 104s [6] and a top voltage of 190 V [4].

Figure 5 shows the horizontal and vertical proton density at the TOTEM 220m roman pots for this case. The beams are shown as a function of time, with the failure occurring at $t=0$, for a stored 7 TeV beam with collision optics ($\beta^*=0.55\text{m}$). Hence the crossing angles and spectrometer dipoles are turned on, the separation bumps are turned off, and the phase 1 collimator apertures are set to the appropriate values, which are given in the appendix of this report. The calculations show the beam orbit rapidly distorts in the horizontal plane, deviates to positive x (as the beam is not bent onto the design orbit as the magnet turns off and drifts to the outside of the ring) and is lost after around 20ms. The beam does not reach the 147m or 220m roman pot apertures in this time. Figure 6 shows the location of the proton losses around the ring, with $s=0$ corresponding to the 220m roman pots. The principle loss spike occurs at the secondary collimator TCSG.A5L7.B1 and, following the arguments in the previous section, the rescattered protons from this collimator will be in the shadow of following collimators. This implies the TOTEM roman pots are in the shadow of the collimation system for a 7 TeV stored beam if the circuit worst-case magnet MB.B12L5.B1 quenches. The implication of beam loss on the secondary collimator TCSG.A5L7, as opposed to a primary collimator, means the error scenario and resulting orbit distortion has reversed the role of the primary and secondary collimators (the jaw different is typically $200\ \mu\text{m}$ at 7 TeV, requiring this level of orbit distortion to achieve this swap). This occurs from the phase advance from the bend to the collimators, and the turn-by-turn phase advance at the TCP and TCSG.

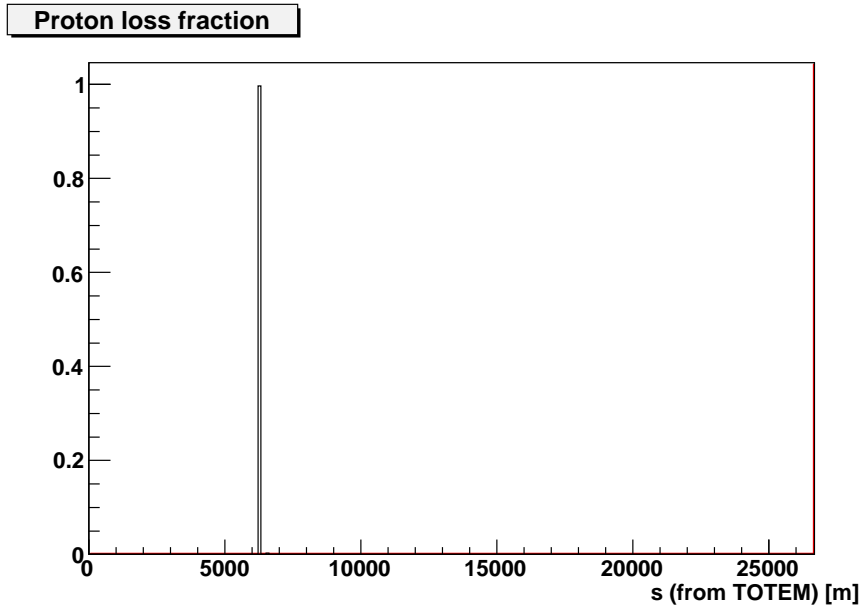


Figure 4: The proton loss map around the ring for a circuit error in RD1.LR5. The calculation was made for a 7 TeV stored beam with collision optics. The loss spike corresponds to loss on a primary collimator.

4.1.3 Quadrupole quench of MQXA.3R5 (Q3)

A quench of the Q3 inner triplet magnet to the right of IP5 (MQXA.3R5) is a potential problem for TOTEM, as this magnet is strong and has an optical relationship to the 220m TOTEM roman pots as to maximise equation 4 (for collision optics at 7 TeV). Furthermore, the non-zero orbit will result in a strong orbit distortion due to the off-axis dipole field. The quench of this magnet would cause the strength to fall as a Gaussian with time constant of 200ms, equation 2, causing β -beat around the ring. Note this would change the ring tune and slightly disturb the phase relationship from Q3 to TOTEM. MQXA.3R5 has a length of 6.37 m, an integrated strength of 0.055577 m^{-1} , and is in the circuit RQX.L5, which powers Q1, Q2 and Q3 on the right-side of the IP. Note the three nested power converters of the final triplet increases the functional complexity of the field decay and the calculations would benefit from the real experiment data [5].

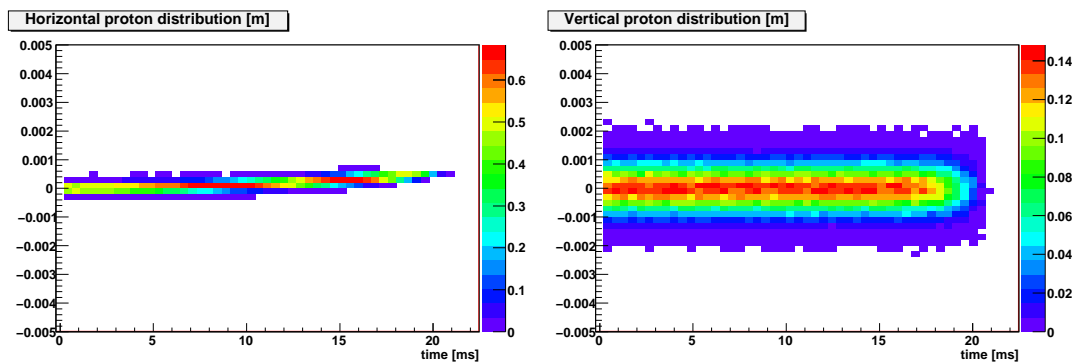


Figure 5: The horizontal and vertical proton distribution at the TOTEM roman pots as a function of time, for a quench in MB.B12L5.B1 and resulting circuit decay in RB.A45. The calculation was made for a 7 TeV stored beam with nominal collision optics.

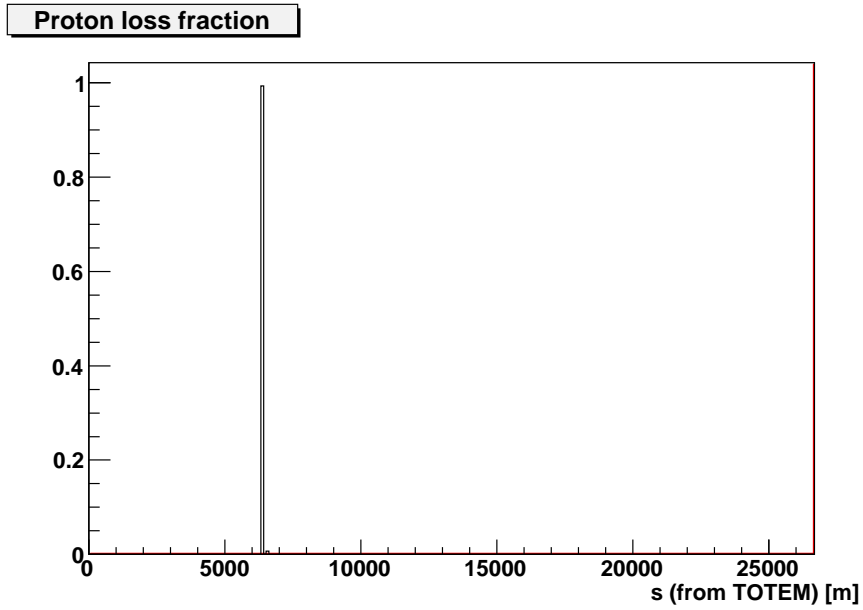


Figure 6: The proton loss map around the ring for a quench in MB.B12L5.B1. The calculation was made for a 7 TeV stored beam with collision optics.

Figure 7 shows the horizontal and vertical proton density in the TOTEM 220m roman pots. The beams are shown as a function of time, with the failure occurring at $t=0$, for a stored 7 TeV beam with collision optics ($\beta^*=0.55$ m). Hence the crossing angles and spectrometer dipoles are turned on, the separation bumps are turned off, and the phase 1 collimator apertures are set to the appropriate values, which are given in the appendix of this report. The calculations shows orbit distortion and β -beating, and the beam is lost after around 20ms onto the primary collimator TCP.B6L7.B1 in the Betatron cleaning section (point 7). The beam does not reach the 147 m or 220 m roman pot apertures in this time and so the TOTEM roman pots are in the shadow of the collimation system for a 7 TeV stored beam if the circuit worst-case quadrupole magnet MQXA.3R5 quenches.

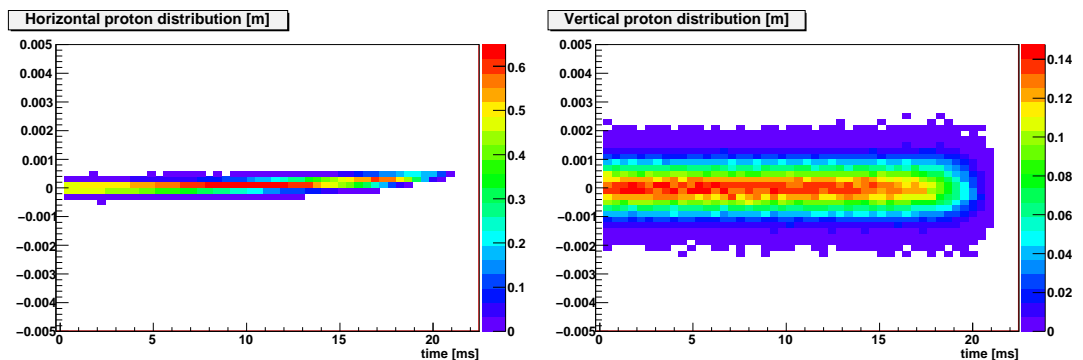


Figure 7: The horizontal and vertical proton distribution at the TOTEM roman pots as a function of time, for a quench in the final triplet quadrupole MQXA.3R5 and resulting circuit decay in RQX.L5. The calculation was made for a 7 TeV stored beam with nominal collision optics.

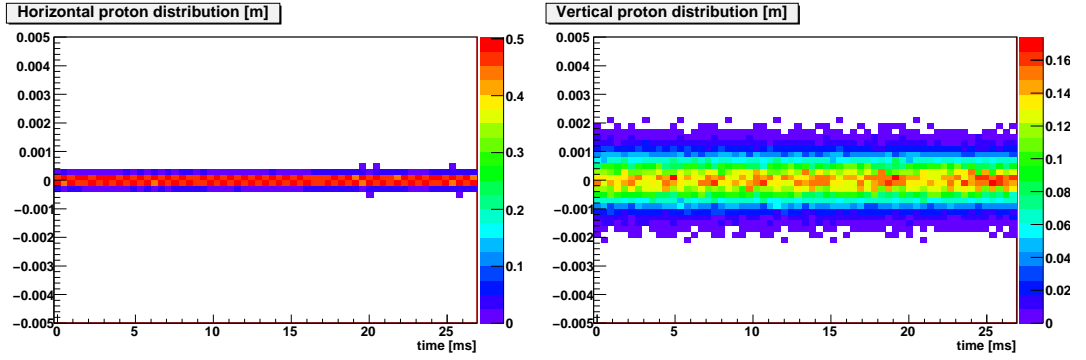


Figure 8: The horizontal and vertical proton distribution at the TOTEM roman pots as a function of time, for a circuit error in RQ5.LR7. The calculation was made for a 7 TeV stored beam with nominal collision optics.

4.1.4 Quadrupole circuit failure in LSS 7

Figure 8 shows the horizontal and vertical proton density in the TOTEM 220m station (RP220), for a worst-case failure of circuit RQ5.LR7. The change of a quadrupole field will result in a β -function change around the ring due to a quadrupole change ΔKL at position k with β -function β_j according to [10]

$$\frac{\Delta\beta(s)}{\beta(s)} = \frac{\sqrt{\beta_j}}{2 \sin(2\pi Q)} (\Delta KL) \cos(2|\Psi(s) - \Psi_j| - 2\pi Q), \quad (4)$$

where $\beta(s)$ denotes the β -function at position s and Q denotes the tune (the horizontal tune is 64.31 for collision optics).

The calculation is done for 7 TeV beam 1, with nominal optics ($\beta^*=0.55\text{m}$) and the circuit decay is modelled with a exponential time constant of 0.611s, with the voltage decaying from the top voltage of 495V (450 V with a 10% safety margin) to zero. The decay of the quadrupole strengths will result in a β -beating around the LHC ring. The beams are shown as a function of time, with the failure occurring at $t=0$, with the TOTEM roman pots at their near-beam configuration at $t=0$. The crossing angles and spectrometer dipoles are turned on, the separation bumps are turned off, and the phase 1 collimator apertures are set to the appropriate values, which are given in the appendix of this report.

The calculations show the beam is only slightly changed after 25ms (300 turns), and there are no beam losses.

4.1.5 Quadrupole quench of MQ.24R3.B1 in sector 34

A possibility of damage to TOTEM arises from a quench in a quadrupole. The damage possibility is low due to the quench detection system and the relatively low β -function at TOTEM. A simulation has been performed of a quench to MQ.24R3.B1 and the resulting quench protection energy extraction in circuit RQD.A34. The quench decay was modelled as a Gaussian with time constant 200ms and the circuit decay of RQD.A34 modelled as an exponential with time constant 40s and top voltage 10.82 V. Note the time constants for the quench protection circuits for quadrupoles (40s) and main dipoles (104s) are different. There is no danger to the TOTEM roman pots to a quench of MQ.24R3.B1 as there is a very slow change to the beam (very small change after 25ms at TOTEM) and so this situation is handled safely by the quench protection and beam dump system.

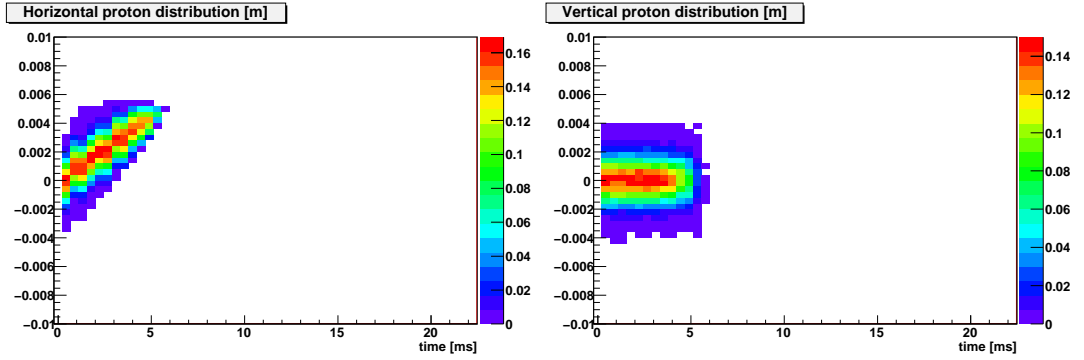


Figure 9: The horizontal and vertical proton distribution at the TOTEM roman pots as a function of time, for a circuit error in RD1.LR1. The calculation was made for a 450 GeV stored beam with nominal collision optics.

4.2 Circulating beam failures for 450 GeV collision optics

In this subsection, the circulating beam failures for TOTEM with 450 GeV collision optics are considered. The long time constant of quenches at this beam energy means the scenarios dangerous for the experiments will be dominated by circuit failure scenarios.

4.2.1 Separation dipole circuit failure in LSS 1 and 5

The circuit RD1.LR1 drives the warm separation dipole D1 in point 1, on both sides of the IR, and the parameters of the circuit are the same as described in section 4.1.1. The circuit decay is modelled with an exponential time constant of 2.038s [4], with the voltage changing from the nominal voltage of 61 V to the top voltage of 1045 V. This change corresponds to the worst case. As for the 7 TeV case the decay of the D1 bend angle will result in an orbit distortion $x(s)$ around the ring.

Figure 9 shows the horizontal and vertical proton density in the TOTEM 220m roman pots, for a worst-case failure of circuit RD1.LR1. The beams are shown as a function of time, with the failure occurring at $t=0$, for a stored 450 GeV beam with collision optics ($\beta^*=10\text{m}$). Hence the crossing angles and spectrometer dipoles are turned on, the separation bumps are turned off, and the phase 1 collimator apertures are set to the values for the phase 1 collimation scheme for 450 GeV, which are given in the appendix of this report. The calculations show the beam orbit rapidly distorts in the horizontal plane to positive x (as the worst case scenario for this circuit is an increase in voltage from 450 GeV nominal voltage to top voltage) and is lost after around 6ms. The beam does not reach the 147m or 220m roman pot apertures in this time.

Figure 10 shows the location of the proton losses around the ring, with $s=0$ corresponding to the 220m roman pots. The principle loss spikes occur at the primary collimator TCP.B6L7.B1, positioned at 6σ , in the Betatron cleaning section, and on the collimator TCSG.6R7.B1, which sees beam after the primary collimator in LSS7. There are a series of collimators positioned after TCP.B6L7.B1, with $\sim 0^\circ$ and 180° phase advances, which will catch any protons re-scattering from this collimator and hence the probability of such a proton surviving to an orbit excursion of 10σ at the TOTEM roman pots is small.

Therefore the TOTEM roman pots are in the shadow of the collimation system for a 450 GeV stored beam if the circuit RD1.LR1 fails, provided the primary collimators are correctly positioned. In common with the 7 TeV case, the results for a failure of the circuit RD1.LR5 are similar to a failure of RD1.LR1 for the 450 GeV case.

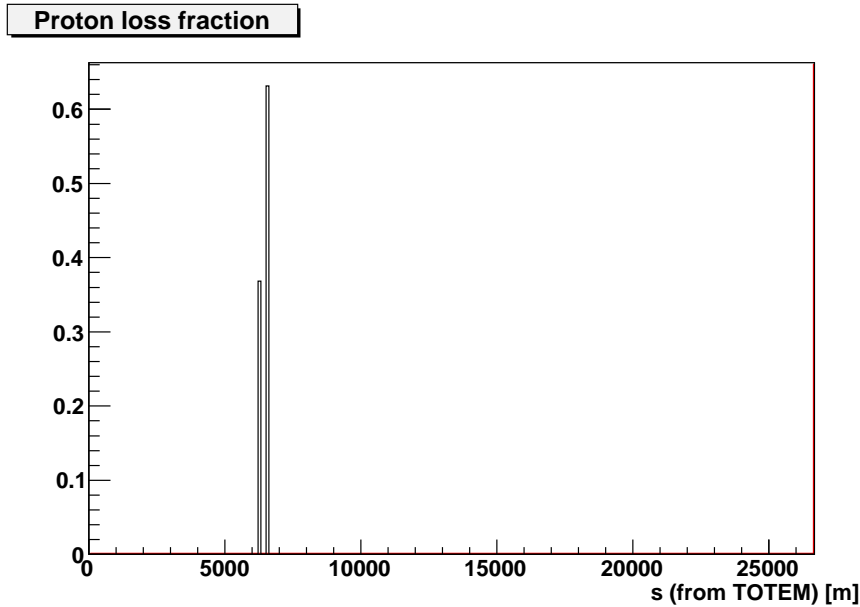


Figure 10: The proton loss map around the ring for a circuit error in RD1.LR1. The calculation was made for a 450 GeV stored beam with collision optics. The major loss spike corresponds to loss on a primary collimator.

4.2.2 Dipole or quadrupole quench

The quench of a dipole or a quadrupole for a 450 GeV circulating beam is a slow failure, due to the time constant of 2000 ms at 450 GeV. To illustrate this, figure 11 shows the horizontal and vertical proton density at TOTEM for a quench of a main dipole in sector 34. The parameters of the quench are the same as in section 4.1.2, apart from the longer quench time constant.

The calculations show the beam is unchanged after 22ms, which is sufficient to dump the beam. Hence there is no danger to the TOTEM experiments from main dipole quenches for a 450 GeV stored beam. Similar conclusions apply to quenches of quadrupoles.

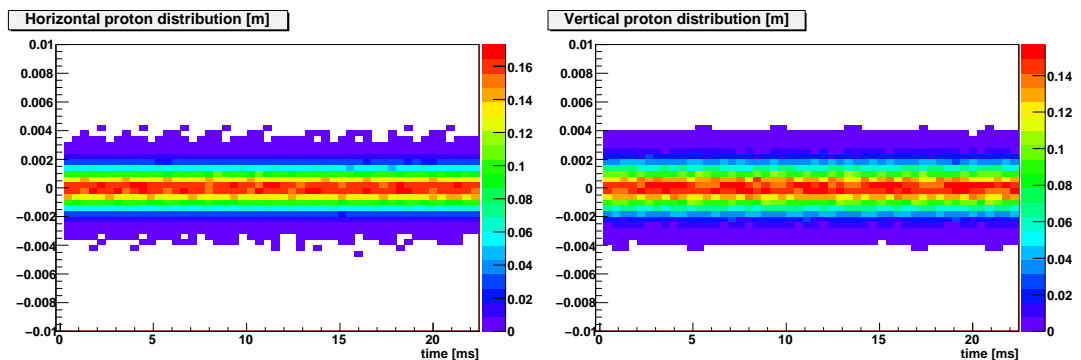


Figure 11: The horizontal and vertical proton distribution at the TOTEM roman pots as a function of time, for a quench of a main bend in sector 45. The calculation was made for a 450 GeV stored beam with nominal collision optics. The long time constant of a quench at 450 GeV means the impact on the beam is on a long timescale.

4.3 Local bumps across TOTEM

The available aperture for the beam in the region of a near-beam experiment can be reduced by the formation of a closed local bump. These bumps can be created across the experiment in a 3-magnet or 4-magnet configuration using the correctors available for global orbit correction, crossing angle and separation bump creation. The bumps can be made by an operator or, albeit unlikely, as a result of an orbit correction algorithm. The 10σ beam distance for TOTEM corresponds to 1mm for the horizontal pot in the 220m station, which is the most vulnerable to local bumps. In this section, bumps at 7 TeV are considered, which is the energy it is most difficult to bump the beam due to the beam rigidity.

The available global orbit correctors have a maximum bend angle of $90 \mu\text{rad}$ (MCBC) or $96 \mu\text{rad}$ (MCBY), and correctors for the crossing angle have a maximum of $1010\mu\text{rad}$ at 450 GeV. Note that some of this strength is used for global orbit correction (typically around $40 \mu\text{rad}$ for the global orbit correctors), leaving the rest available for local bumps.

The left-hand plot of figure 12 shows a 3-magnet horizontal closed bump across the 220m TOTEM station using the correctors MCBCH.5R5, MCBCH.7R5 and MCBCH.9R5. The bump is opened at 199m from the IP, with MCBCH.5R5 set to $26 \mu\text{rad}$ (it's nominal value is $-22 \mu\text{rad}$), and closed at 348m from the IP, with MCBCH.7R5 set to $41 \mu\text{rad}$ and MCBCH.9R5 set to $31 \mu\text{rad}$. The orbit change just after 260m is due to a horizontal focusing quadrupole Q7 in the middle of the bump. This bump, with correctors strengths consistent with the orbit correction creates a horizontal orbit distortion of +1mm at the 220m TOTEM station, sending the beam into the horizontal pot on the outside edge of the beam pipe. The right-hand plot in figure 12 shows the possible vertical bumps at 220m, which cannot impact the vertical detectors if the vertical correctors are kept within their limits (this excludes the allowance of global orbit correction, which provides a further safety margin). The correctors used to apply the local bumps across TOTEM are slow, and change at 0.5 A/s and so a bump of 1mm at TOTEM will be applied over a long timescale of many seconds.

The possibilities for detection and interlocking of such a closed bump are

1. The corrector magnets around the near-beam detectors could be interlocked, to permit only a small relative change once the orbit is corrected and the moveable detectors flag is enabled.
2. Interlock software could monitor the near-beam detector distance to the current beam orbit, giving a warning if some mechanism reduces the available aperture at a near-beam detector.
3. The downstream BLMs may see a signal when the bump is being applied, although the time-scale needs to be calculated.

The danger to near-beam experiments from local bumps is known to the Machine Protection Panel (MPP). A further dangerous situation is the combination of a local bump across an experiment, reducing the available aperture for beam, combine with a fast failure of a dipole or quadrupole around the ring. This could lead to beam loss in the bumped region before loss on the collimation system, as concluded for the calculations earlier in this section. However, this combined scenario is unlikely and would be mitigated by the bump detection mechanisms discussed in this section.

Note, bumps at 450 GeV across TOTEM are easier and quicker to create than the 7 TeV case, increasing the need for detection mechanisms and interlocks. Finally, it should be noted that there are many correctors around TOTEM, and many ways to create

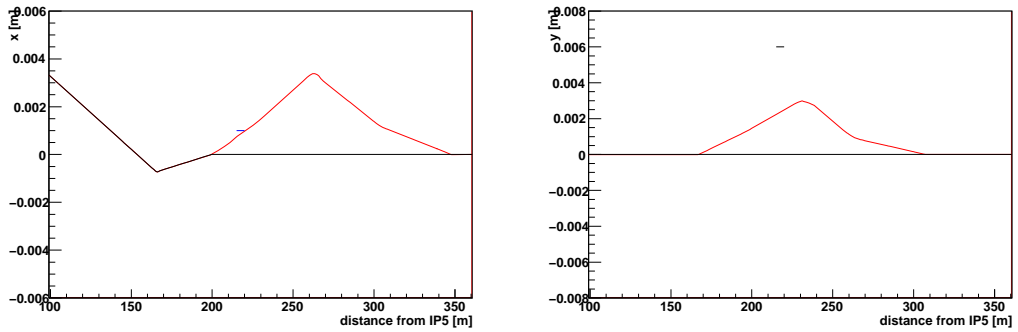


Figure 12: The formation of horizontal and vertical local closed bumps across the TOTEM 220m station. The available correctors can make a dangerous horizontal bump, but not a vertical bump. The black line shows the ideal orbit, the red line shows the bumped orbit and the blue line denotes the physical boundary of the TOTEM pot.

closed bumps across the experiment. The subsequent reduction of aperture in this region is potentially very dangerous to the near-beam detectors.

5 LHCb (the VELO)

In this section accident scenarios for the VELO [11] of LHCb (IR8) for a 450 GeV stored beam with collision optics are considered. The LHCb VELO (VERTex LOcator) is a moveable near-beam detector to provide precise track reconstruction close to the interaction point to measure the vertices of b-hadron decays. The detector will sit in a parked position of 30mm from the beam, and when a stable beam is established, will move to 5mm from the beam. This closed position forms a considerable aperture restriction. The studies in this section will focus on beam accident scenarios for a closed VELO and a 450 GeV stored beam with collision optics. This is expected to be the worst stored beam case for the VELO machine protection, due to the largest IP beam size and the low beam rigidity. As for the case of magnet quenches at 450 GeV with TOTEM described in section 4.2, the failure scenarios for the VELO with magnet quenches are expected to give slow beam size changes at the VELO and should provide no danger for the experiment.

To study the VELO, the 5mm aperture restriction was included in the 450 GeV runs in the previous section. For the worst-case scenarios considered, the loss was confined to the primary and secondary collimators, as shown in the TOTEM 450 GeV analysis. As an illustration of the beam dynamics at the VELO location, the case of separation dipole circuit failure in LSS 1 is considered explicitly in the next section. Other cases, such as the those for the VELO found in [3], have been performed and identical results obtained.

5.1 Circulating beam failure: separation dipole circuit failure in LSS 1

Figure 13 shows the horizontal and vertical proton density at the VELO at IR8, for a worst-case failure of circuit RD1.LR1. The circuit decay is modelled with an exponential time constant of 2.038s, with the voltage rising from the nominal voltage of 61 V to their maximum of 1045 V (950 V with a 10% safety margin).

The beams are shown as a function of time, with the failure occurring at $t=0$, for a stored 450 GeV beam with collision optics. Hence the crossing angles and spectrometer dipoles are turned on, and the separation bumps are turned off. The phase 1 collimator apertures are set to the appropriate values, which are given in the appendix of this report. The calculations show the beam orbit rapidly distorts in the horizontal plane, deviates

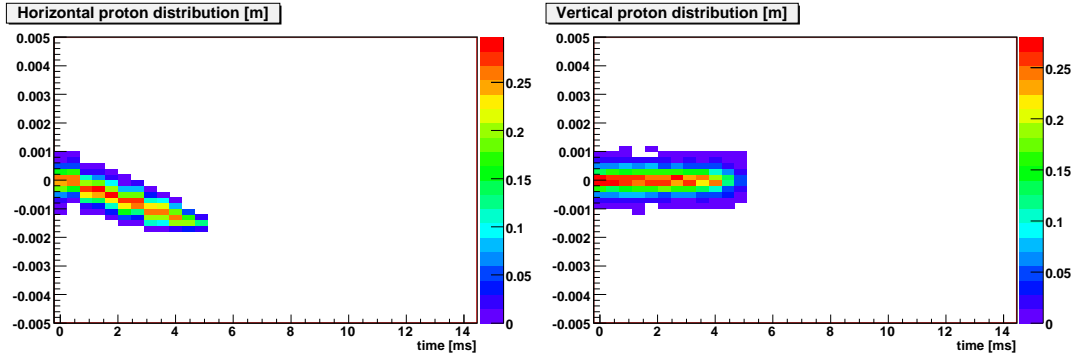


Figure 13: The horizontal and vertical proton distribution at the VELO as a function of time, for a circuit error in RD1.LR1. The calculation was made for a 450 GeV stored beam with collision optics.

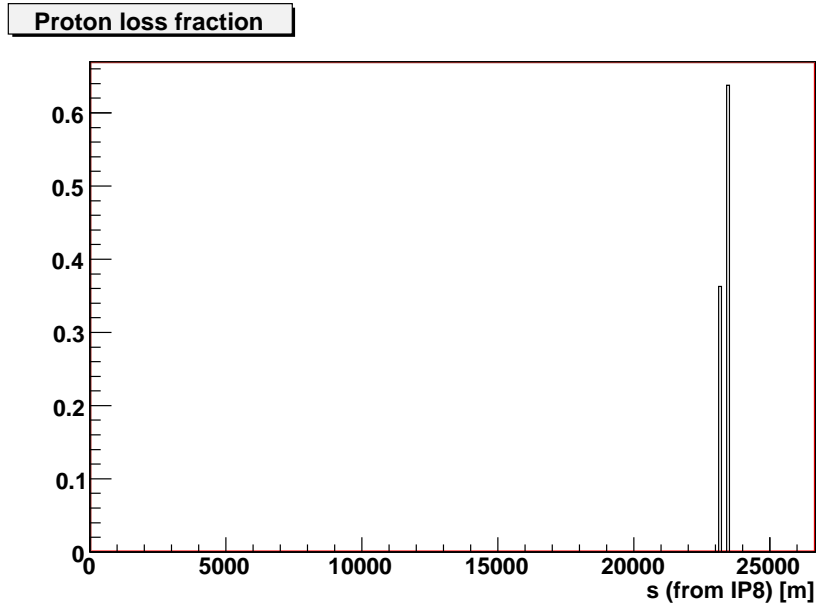


Figure 14: The proton loss map around the ring for a circuit error in RD1.LR1. The calculation was made for a 450 GeV stored beam with collision optics.

to negative x and is lost after around 5ms. The beam does not reach the 5mm aperture of the VELO in this time. Figure 14 shows the location of the proton losses around the ring, with $s=0$ corresponding to IP8, which occur in the betatron cleaning section. The principle loss spikes occur at 23136m, corresponding to loss on TCP.B6L7.B1 and at 23484m, corresponding to loss on TCSG.6R7.B1. These losses are consistent with figure 10. Therefore the closed VELO is in the shadow of the collimation system for a 450 GeV stored beam, if the circuit RD1.LR1 fails. A similar conclusion can be drawn for the failure of RD1.LR5, as for the TOTEM studies in section 4.

5.2 Local bumps across LHCb

The small aperture of a closed VELO means the possibility exists to make local closed bumps across the experiment and reduce the available aperture at the VELO. The closed position of 5mm means bump creation is harder than for the 220m TOTEM pots, and very difficult with a single corrector before the VELO. However it is possible to make

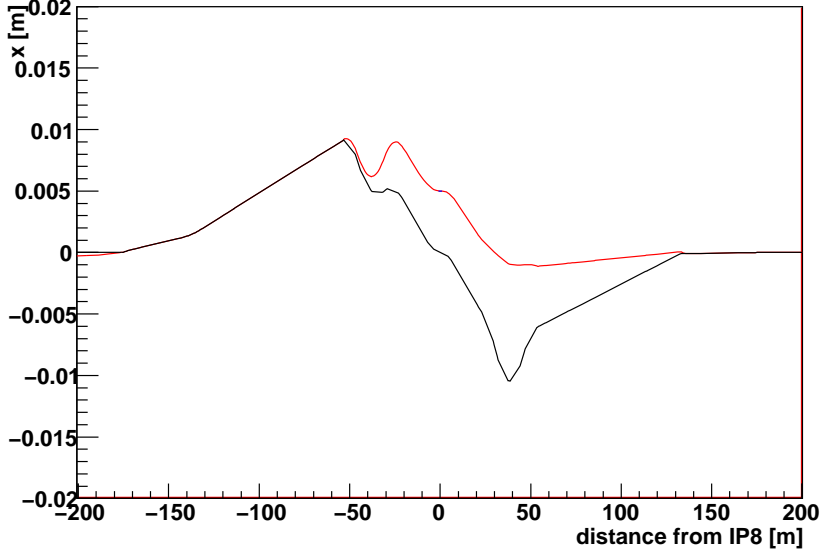


Figure 15: The formation of a horizontal local closed bumps across the LHCb VELO. The available correctors can make a dangerous horizontal bump of +5mm. The black line shows the ideal orbit, the red line shows the bumped orbit and the blue line denotes the physical boundary of the VELO

a 5mm bump for a 7 TeV stored beam (which is the hardest case to make a bump) across the VELO using two upstream MCBX correctors acting coherently, and closed downstream of the VELO. An example of such a bump is shown in figure 15, which shows a 5mm horizontal bump at the VELO which is opened with the correctors MCBX.3L8 and MCBX.2L8, and closed at the corrector MCBYH.B4R8.B1 using the intervening correctors. Note that this bump is created with the two opening correctors close to their maximum current (for a 7 TeV beam).

This bump reduces the available aperture at the VELO, can cause direct beam strike and makes the VELO more vulnerable to the circulating beam accident scenarios discussed in this report. The comments made for TOTEM bumps in section 4.3 apply to the bumps across VELO, particularly regarding the speed of the bump, the possible detection mechanisms and the many possible ways to create bumps across the experiment.

6 Conclusion

This report has focused on beam accident scenarios with a circulation beam with collision optics which can affect the near-beam detectors of TOTEM and LHCb. The scenarios considered include the failure of power converters, the quench of quadrupoles and dipoles and the formation of local bumps across the experiment. All studies were done for 7 TeV and 450 GeV.

For the case of TOTEM, a worst-case range of scenarios for the 7 TeV stored beam was considered. It was found in all cases that the roman pots of TOTEM were in the shadow of the collimation system, and did not receive beam in the cases considered. This conclusion relies on the correct positioning and alignment of the collimation system. For the 450 GeV case, similar conclusions were drawn. It was shown, however, that it is possible to create local bumps across TOTEM which reduces the available aperture and could cause a potential beam strike. There are several ways to prevent this situation,

including relative current interlocks, on-line monitoring of the beam orbit at TOTEM and using downstream BLMs to detect the aperture reduction.

The studies for the VELO were performed at 450 GeV for the circulating beam. Again, the detector was in the shadow of the collimation system for all cases considered. For local bumps across the VELO, this is possible at both 7 TeV and 450 GeV, reducing the available aperture. This can be prevented with on-line monitoring of orbit.

In summary, the near-beam detectors rely on the correct positioning of the primary and secondary collimators for protection against accident scenarios. However, the aperture at the experiments can be reduced with local closed bumps, which requires interlocking, detection and monitoring.

The study of on-line orbit monitoring for TOTEM, LHCb VELO and other near-beam experiments is a possible way to extend the work in this report. A further extension could be to go beyond the linear element field changes considered in this report, and study non-linear element failure. For example, a sextupole circuit failure would lead to change in chromaticity and tune spread.

The effects of proton rescattering at collimators and the potential impact on the beam safety of the near-beam detectors remains to be studied. Protons lost on collimators are assumed to be no danger to TOTEM in this work, by consideration of the phase relationships between TOTEM and the collimators in points 3 and 7. A more detailed study would check these rescattered protons, which may survive several turns as they diffuse in impact parameter space up the collimators, using the code Sixtrack. Although a proton rescattering from a collimator and reaching a near-beam experiment is unlikely, this study would provide a cross-check of the phase arguments used, and is left to a future collaboration with the collimation group.

Acknowledgement

The author would like to acknowledge Daniela Macina and Emmanuel Tsesselis in the TS/LEA group for helpful conversations and advice, Jorg Wenninger and Rudiger Schmidt for advice on the machine aspects of this work, and Andres Gomez Alonso for many helpful discussions and useful assistance.

References

- [1] R. Schmidt and J. Wenninger, the Proceedings of 2005 Particle Accelerator Conference, Knoxville, Tennessee
- [2] V. Kain, LHC-Project-Note 322, CERN, Geneva, 2003
- [3] A. Gomez Alonso, PhD thesis (under preparation)
- [4] <http://layout.web.cern.ch/layout/>
- [5] M. Koratzinos, Private communication
- [6] The LHC design report, CERN-2004-003 (2004)
- [7] The MADX program, <http://www.cern.ch/mad>
- [8] ROOT, <http://root.cern.ch/>
- [9] The TOTEM technical design report, CERN-LHCC-2004-002 (2004)
- [10] A. Chao (ed.), The handbook of accelerator physics and engineering, World Scientific (2002)
- [11] LHCb TDR 5 CERN/LHCC 2001-0011
- [12] I. Agapov *et al*, the Proceedings of 2007 Particle Accelerator Conference, Albuquerque, New Mexico

A Primary and secondary collimator settings used in this work

The settings of the primary collimators used in this work for the 450 GeV and 7 TeV beam studies are listed in this appendix for future reference. The parameter ALPHA denotes the rotation angle of the jaws, and the settings given are the half-gap.

A.1 450 GeV with collision optics

– Point 3

TCP.6L3.B1, RECTANGLE, APERTURE={ 0.007848,0.04 }
TCSG.5L3.B1, RECTANGLE, APERTURE={ 0.005877, 0.04 }
TCSG.4R3.B1, RECTANGLE, APERTURE={ 0.004066, 0.04 }
TCSG.A5R3.B1, RECTANGLE, APERTURE={ 0.005261, 0.04 }, ALPHA=2.980
TCSG.B5R3.B1, RECTANGLE, APERTURE={ 0.005896, 0.04 }, ALPHA=0.189

– Point 7

TCP.D6L7.B1, RECTANGLE, APERTURE={ 0.04, 0.0042634 }; ALPHA=1.5707
TCP.C6L7.B1, RECTANGLE, APERTURE={ 0.006037, 0.04 }
TCP.B6L7.B1, RECTANGLE, APERTURE={ 0.005044, 0.04 }, ALPHA=2.215
TCSG.A6L7.B1, RECTANGLE, APERTURE={ 0.006087, 0.04 }, ALPHA=2.463
TCSG.A5L7.B1, RECTANGLE, APERTURE={ 0.007374,0.04 }, ALPHA=0.710
TCSG.A4L7.B1, RECTANGLE, APERTURE={ 0.006650, 0.04 }, ALPHA=2.349
TCSG.A4R7.B1, RECTANGLE, APERTURE={ 0.0066798,0.04 }, ALPHA=0.808
TCSG.6R7.B1, RECTANGLE, APERTURE={ 0.01057,0.04 }, ALPHA=0.009

A.2 7 TeV with collision optics

– Point 3

TCP.6L3.B1, RECTANGLE, APERTURE={ 0.003881, 0.04 }
TCSG.5L3.B1, RECTANGLE, APERTURE={ 0.002999, 0.04 }
TCSG.4R3.B1, RECTANGLE, APERTURE={ 0.002068, 0.04 }
TCSG.A5R3.B1, RECTANGLE, APERTURE={ 0.002686, 0.04 }, ALPHA=2.980
TCSG.B5R3.B1, RECTANGLE, APERTURE={ 0.003011, 0.04 }, ALPHA=0.189

– Point 7

TCP.D6L7.B1, RECTANGLE, APERTURE={ 0.04,0.001153 }, ALPHA=1.5707
TCP.C6L7.B1, RECTANGLE, APERTURE={ 0.001703,0.04 }
TCP.B6L7.B1, RECTANGLE, APERTURE={ 0.001393,0.04 }, ALPHA=2.225
TCSG.A6L7.B1, RECTANGLE, APERTURE={ 0.001658, 0.04 }, ALPHA=2.463
TCSG.A5L7.B1, RECTANGLE, APERTURE={ 0.001982,0.04 }, ALPHA=0.710
TCSG.A4L7.B1, RECTANGLE, APERTURE={ 0.001826,0.04 }, ALPHA=2.349
TCSG.A4R7.B1, RECTANGLE, APERTURE={ 0.001838,0.04 }, ALPHA=0.808
TCSG.6R7.B1, RECTANGLE, APERTURE={ 0.002949, 0.04 }, ALPHA=0.009